

Functional characterization of three intercalated cell subtypes in the rabbit outer cortical collecting duct.

C Emmons, I Kurtz

J Clin Invest. 1994;**93**(1):417-423. <https://doi.org/10.1172/JCI116976>.

Research Article

The distribution of Na(+)-independent Cl(-)-HCO₃⁻ exchange was studied in individual intercalated cells from in vitro perfused rabbit outer CCDs using dual excitation laser scanning confocal microscopy by measuring the pHi response to sequential removal of Cl⁻ from both sides of the tubule. Three patterns of intracellular pH (pHi) response were observed. 39% of intercalated cells had only apical Cl(-)-HCO₃⁻ exchange (beta cell), 4% had only basolateral Cl(-)-HCO₃⁻ exchange (alpha cell), and 57% had both apical and basolateral Cl(-)-HCO₃⁻ exchange (gamma cell). Valinomycin-high K⁺ voltage clamping had no effect on the pHi response of intercalated cells with bilateral Cl(-)-HCO₃⁻ exchange. Although the mean rates of dpHi/dt following apical Cl⁻ removal were similar in beta cells compared to gamma cells, a wide range of apical rates was seen among individual beta and gamma intercalated cells. Neither the apical nor the basolateral Cl(-)-HCO₃⁻ exchanger in gamma cells was inhibited by 0.5 mM H₂DIDS. Binding of apical peanut lectin was seen both in beta cells and in gamma cells. In 41% of CCDs with four to seven intercalated cells studied, all intercalated cells were of the same subtype. We conclude that the majority of intercalated cells from the rabbit outer CCD have both apical and basolateral Na(+)-independent Cl(-)-HCO₃⁻ exchangers (gamma cells), which are stilbene-insensitive. Intercalated cells with only basolateral Cl(-)-HCO₃⁻ exchange are very uncommon [...]

Find the latest version:

<https://jci.me/116976/pdf>



Functional Characterization of Three Intercalated Cell Subtypes in the Rabbit Outer Cortical Collecting Duct

Cheryl Emmons** and Ira Kurtz†

Nephrology Division, Department of Medicine, *Wadsworth Veterans Administration Medical Center, Los Angeles, California 90024; and †University of California at Los Angeles Center for the Health Sciences, Los Angeles, California 90024

Abstract

The distribution of Na⁺-independent Cl⁻-HCO₃⁻ exchange was studied in individual intercalated cells from in vitro perfused rabbit outer CCDs using dual excitation laser scanning confocal microscopy by measuring the pHi response to sequential removal of Cl⁻ from both sides of the tubule. Three patterns of intracellular pH (pHi) response were observed. 39% of intercalated cells had only apical Cl⁻-HCO₃⁻ exchange (β cell), 4% had only basolateral Cl⁻-HCO₃⁻ exchange (α cell), and 57% had both apical and basolateral Cl⁻-HCO₃⁻ exchange (γ cell). Valinomycin-high K⁺ voltage clamping had no effect on the pHi response of intercalated cells with bilateral Cl⁻-HCO₃⁻ exchange. Although the mean rates of dpHi/dt following apical Cl⁻ removal were similar in β cells compared to γ cells, a wide range of apical rates was seen among individual β and γ intercalated cells. Neither the apical nor the basolateral Cl⁻-HCO₃⁻ exchanger in γ cells was inhibited by 0.5 mM H₂DIDS. Binding of apical peanut lectin was seen both in β cells and in γ cells. In 41% of CCDs with four to seven intercalated cells studied, all intercalated cells were of the same subtype. We conclude that the majority of intercalated cells from the rabbit outer CCD have both apical and basolateral Na⁺-independent Cl⁻-HCO₃⁻ exchangers (γ cells), which are stilbene-insensitive. Intercalated cells with only basolateral Cl⁻-HCO₃⁻ exchange are very uncommon in the rabbit outer CCD. There is a tendency for all intercalated cells in a given rabbit outer CCD to be of the same subtype (either all β cells or all γ cells), suggesting the presence of CCD intertubule heterogeneity at the same cortical level. This finding may account for intertubule differences in transepithelial H⁺-base transport. (*J. Clin. Invest.* 1994; 93:417–423.) Key words: acid-base • intracellular pH • intercalated cells • confocal microscopy • anion exchange

Introduction

The cortical collecting duct (CCD)¹ is a heterogeneous epithelium composed of two main cell types: principal cells and intercalated

Portions of this work were presented at the annual meeting of the American Society of Nephrology, 20–21 November, 1991, Baltimore, MD, and were published in abstract form (1991. *J. Am. Soc. Nephrol.* 2:699).

Address correspondence to Dr. Cheryl Emmons, Nephrology Division, UCLA Center for the Health Sciences, 10833 Le Conte Boulevard, Factor 7-453, Los Angeles, CA 90024.

Received for publication 7 April 1993 and in revised form 11 August 1993.

1. Abbreviations used in this paper: BCECF-AM, acetoxymethyl ester of 2',7'-bis-(2-carboxyethyl)-5-(and-6)carboxyfluorescein; CCD, cor-

cells (1). It is the latter group of cells that is believed to mediate transepithelial CCD acid-base transport. Intercalated cells have been traditionally divided into two types based on their morphology, antibody binding properties, and acid-base transport characteristics. Bicarbonate secretion is attributed to β intercalated cells, which have been modeled with an apical Na⁺-independent Cl⁻-HCO₃⁻-exchanger, a basolateral H⁺-ATPase, and a basolateral Cl⁻ channel. α intercalated cells are thought to effect CCD HCO₃⁻ absorption and are modeled with an apical H⁺-ATPase, a basolateral Na⁺-independent Cl⁻-HCO₃⁻ exchanger and a basolateral Cl⁻ channel (2–8). In addition, apical lectin binding has been considered a characteristic marker for β cells (3, 9, 13). Although β cells do not bind antibodies to the erythrocyte anion exchanger band 3, α cells do exhibit basolateral staining (9, 15, 19). However, recent morphologic and immunocytochemical studies have identified “hybrid” cells with features attributed to both intercalated cell subtypes (14–17, 29). The functional significance of these findings is unknown.

Much of the current understanding of CCD acid-base transport characteristics is derived from whole tubule studies. The heterogeneous nature of the CCD makes it difficult to ascertain function on a single-cell level. Optical approaches have been used to study single-cell H⁺-base transport; however, the cylindrical geometry of the tubule has made optical studies of individual cells troublesome due to the acquisition of out-of-focus information. This difficulty can be overcome using confocal microscopy (10). The present study was undertaken to functionally characterize the distribution of Na⁺-independent Cl⁻-HCO₃⁻ exchange in single intercalated cells in the rabbit outer CCD using dual excitation laser scanning confocal microscopy. The results indicate that the majority of rabbit outer CCD intercalated cells do not fit either of the two classic intercalated cell models.

Methods

Tubule perfusion. Male New Zealand White rabbits weighing 4 lbs and with free access to rabbit chow (Prolab; Agway Country Foods, Inc., Syracuse, NY) were killed by cervical dislocation. The left kidney was removed, cut in coronal sections, and placed in chilled solution 1 (Table I). Cortical collecting ducts were dissected from the outer mm of cortex, with the most superficial end starting at the most distal connecting tubule arcade into the collecting duct (11). The tubule was transferred to a 100-μl laminar flow chamber and the peritubular bathing solution was exchanged at a rate of 2 ml/min.

Solutions. The solutions used in the study are listed in Table I. All were Na⁺-free (tetramethylammonium replacement) to eliminate any contribution of Na⁺-dependent transport processes to alterations in pHi. Solution 1 was used for the dissection solution. Solution 2 was the initial perfusing and bathing solution, except where specified. Solution 3 was free of Cl⁻ (gluconate replacement). Solutions 4 and 5 were used

tical collecting duct; 6-CF, 6-carboxylfluorescein; H₂DIDS, 4,4'-diisothiocyanatodihydrostilbene-2,2'-disulfonic acid; pHi, intracellular pH.

Table I. List of Solutions Used in the Study

Solutions	1	2	3	4	5	6
Tetramethylammonium hydroxide	0	0	115	0	0	0
Tetramethylammonium chloride	140	115	0	20	0	0
Gluconic acid lactone	0	0	115	0	20	0
Tetramethylammonium bicarbonate	0	25	25	25	25	0
KCl	0	0	0	95	0	115
K ₂ HPO ₄	2.5	2.5	2.5	2.5	2.5	2.5
K-gluconate	0	0	0	0	95	0
CaCl ₂	1	1	0	1	0	1
Ca-gluconate	0	0	3.5	0	3.5	0
MgCl ₂	1	1	0	1	0	1
Mg-gluconate	0	0	1	0	1	0
Hepes acid	5	0	0	0	0	5
L-alanine	5	5	5	5	5	5
Glucose	5	5	5	5	5	5

All concentrations are in mmol/liter.

for the valinomycin experiments, and solution 6 was used for calibration of pH_i with $10 \mu M$ nigericin added. The HCO_3^- -containing solutions were bubbled with 6.5% CO_2 and 93.5% O_2 , while the Hepes-containing solutions were bubbled with 100% O_2 . Tetramethylammonium bicarbonate was made by bubbling tetramethylammonium hydroxide with 100% CO_2 . Glass tubing, surrounded by heated water jackets, connected the solution reservoirs and the perfusion chamber to prevent any CO_2 or temperature loss. The pH of all solutions was 7.4, and all experiments were performed at $37^\circ C$.

pH_i measurements/confocal imaging. To measure pH_i , $5 \mu M$ acetoxymethyl ester of 2',7'-bis(2-carboxyethyl)-5-(and -6)carboxyfluorescein (BCECF-AM) was added to the appropriate perfusate solution for 15 min, resulting in selective dye loading of only the intercalated cells and confirmed by "rough" surface appearance with transmission imaging (12). The perfusate was then changed to the appropriate dye-free solution for 10 min before any data was recorded. The fluorescent measurements were accomplished with the use of a dual-excitation laser-scanning inverted confocal fluorescent microscope, as previously described (10). The previous methodology was modified as follows. A laser-scanning system (model MRC600; BioRad Laboratories, Richmond, CA) was coupled to the side port of a Diaphot inverted microscope (Nikon Inc., Melville, NY). An argon laser (model 5424A; Ion Laser Technology, Inc., Salt Lake City, UT) was used for the 488-nm excitation and a helium-cadmium laser (model 4214NB; Liconix, Santa Clara, CA) provided the 442-nm excitation. A $40\times$ fluorite objective (N.A. 0.8; Nikon Inc.) was used in all experiments. pH_i was measured from an area of cytoplasm of ~ 3 to $5 \mu m$ in diameter in up to 7 intercalated cells along a $250\text{-}\mu m$ length of tubule (UMANS software; BioRad Laboratories). A zoom factor of 2.5 was used to obtain images of the tubule (final magnification of 800). A computer-driven electronic shutter (Vincent Associates, Rochester, NY) in front of each laser limited the duration of laser exposure to 1 s per ratio. Excitation ratio measurements were taken every 5 s after a solution change and the rate of change of pH_i (dpH_i/dt) was evaluated in the initial 20 s.

Materials. 4,4'-diisothiocyanatodihydrostilbene-2,2'-disulfonic acid (H_2DIDS) and BCECF-AM were from Molecular Probes, Inc. (Eugene, OR). Tetramethylammonium hydroxide was from Fisher Scientific (Fair Lawn, NJ) and all other chemicals were from Sigma Chemical Co. (St. Louis, MO).

Statistics. All results are reported as mean \pm SEM. Student's unpaired t test was used to compare results from two group means obtained from separate tubules. Student's paired t test was used to compare results of inhibitor studies in the same tubule. Statistical significance was accepted at the $P \leq 0.05$ level.

Results

Patterns of Na^+ -independent Cl^- - HCO_3^- exchange in CCD intercalated cells. In the initial experiments, Cl^- was replaced with gluconate (solution 3) sequentially on both sides of the tubule. This protocol was examined in 309 intercalated cells from 72 CCDs. Three patterns of pH_i response were seen (Figs. 1–3). One pattern is illustrated in Fig. 1. In this particular cell, the initial pH_i was 6.92. Removal of Cl^- from the lumen resulted in an increase in pH_i to a steady-state value of 7.05. pH_i was not altered further with removal of Cl^- from the bath. This pattern of Cl^- -base exchange was seen in 39% of the intercalated cells studied with this protocol and is consistent with the existing model of the β intercalated cell, an intercalated cell with only apical anion exchange. In these intercalated cells with only apical Cl^- -base exchange, mean baseline pH_i was 6.94 ± 0.06 , mean dpH_i/dt after apical Cl^- removal was 1.16 ± 0.17 pH_i/min , and mean ΔpH_i was 0.33 ± 0.04 pH_i units.

A second pattern of pH_i response is seen in Fig. 2. pH_i was

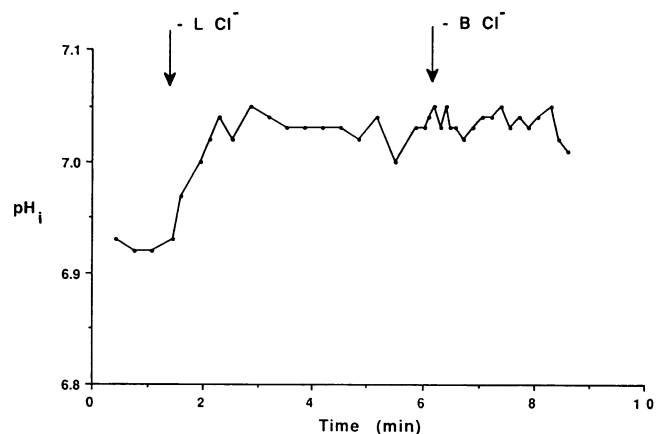


Figure 1. pH_i response to sequential lumen and basolateral Cl^- removal (pattern 1). Removal of lumen Cl^- results in intracellular alkalinization, with no further change in pH_i from removal of bath Cl^- . These results are compatible with the classic β cell model.

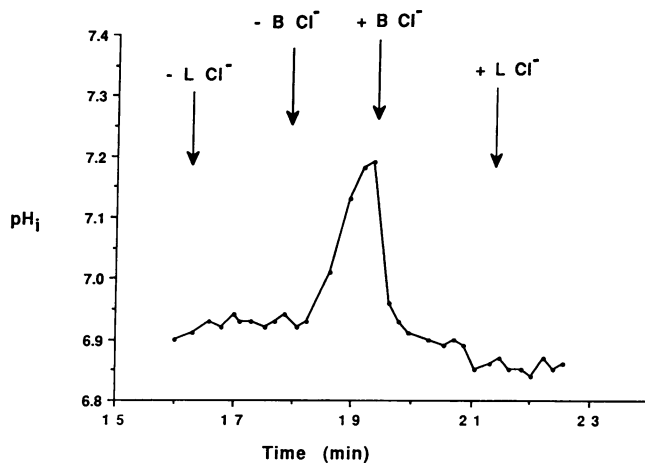


Figure 2. pH_i response to sequential lumen and basolateral Cl^- removal (pattern 2). pH_i was unchanged after removal of lumen Cl^- and increased in response to removal of bath Cl^- . This result was rarely seen and is compatible with the classic α cell model.

not altered with removal of lumen Cl^- . However, removal of bath Cl^- resulted in an increase in pH_i from 6.92 to 7.20. This pattern of Cl^- -base exchange is consistent with the current model of the α intercalated cell, one with only basolateral anion exchange. This pattern of Cl^- -base exchange was seen in only 4% of CCD intercalated cells, and occurred so infrequently that this cell type could not be studied in any detail.

A third pattern of pH_i response is seen in Fig. 3. In this cell, baseline pH_i was 7.02. Removal of lumen Cl^- caused alkalinization with subsequent stabilization of pH_i at 7.21. In contrast to Fig. 1, removal of basolateral Cl^- in this cell caused further alkalinization to pH_i 7.30, with a decrease in pH_i when Cl^- was readded to the bath. This tracing is not consistent with either the current α or β intercalated cell models. In a separate study (Fig. 4), bath Cl^- was removed initially, resulting in an increase in pH_i to 7.20. Readdition of bath Cl^- caused the pH_i to return to its baseline, 7.05. After removal of lumen Cl^- , pH_i

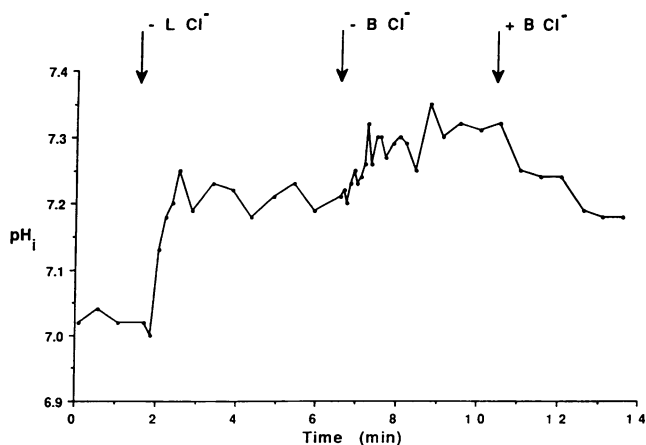


Figure 3. pH_i response to sequential lumen and basolateral Cl^- removal (pattern 3). After removal of lumen Cl^- , pH_i increased followed by a further cell alkalinization in response to removal of bath Cl^- . These findings indicate the presence of bilateral Cl^- -base exchange. This new intercalated cell subtype is designated as the γ cell.

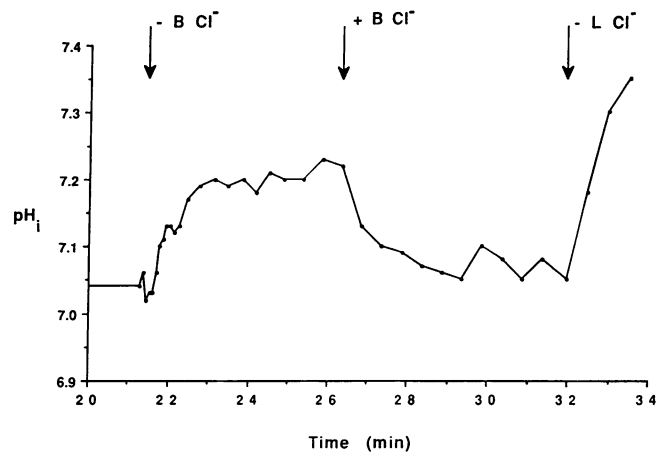


Figure 4. pH_i response to sequential lumen and basolateral Cl^- removal (pattern 3). Removal of bath Cl^- caused pH_i to increase. Readdition of bath Cl^- resulted in recovery of pH_i . Removal of lumen Cl^- resulted in an increase in pH_i .

increased to 7.35. The sequence of Cl^- removal made no difference in the pH_i response seen. 57% of the intercalated cells studied demonstrated this pattern of an increase in pH_i after both bath and lumen Cl^- removal. These results are best explained by an intercalated cell with bilateral Cl^- -base exchangers (γ cell). In these intercalated cells with bilateral Cl^- -base exchangers, baseline pH_i was 7.06 ± 0.06 . The dpH_i/dt after apical Cl^- removal was 1.25 ± 0.18 with a ΔpH_i of 0.30 ± 0.04 . The dpH_i/dt after basolateral Cl^- removal was 0.86 ± 0.15 with a ΔpH_i of 0.29 ± 0.05 (all NS vs. intercalated cells with only apical anion exchange).

Further experiments were done in separate tubules to eliminate the possibility of any conductive pathway as a cause for the apical and basolateral Cl^- -induced pH_i changes. The protocol was repeated in the presence of $5 \mu M$ luminal and basolateral high K^+ -valinomycin solutions (solution 4, Table I) to clamp the apical and basolateral membrane potential. The results of such an experiment are seen in Fig. 5. In this cell, removal of lumen Cl^- (solution 5) resulted in intracellular alkalinization, as expected in a cell with apical anion exchange. Removal of bath Cl^- resulted in further alkalinization, which was reversible with readdition of Cl^- to the bath. The dpH_i/dt after apical Cl^- removal in the presence of high K^+ -valinomycin solutions in 32 intercalated cells with bilateral Cl^- -base exchange from 12 tubules was 0.92 ± 0.15 with a ΔpH_i of 0.25 ± 0.05 . The dpH_i/dt after basolateral Cl^- removal was 1.13 ± 0.16 with a ΔpH_i of 0.24 ± 0.04 .

Although the mean rates of dpH_i/dt in response to luminal Cl^- removal are similar for both β and γ intercalated cell subtypes, an array of rates was seen, as depicted in Fig. 6. These data suggest that within a given intercalated cell subtype (β cells with only apical Cl^- -base exchange and γ cells with bilateral Cl^- -base exchange), there is a wide range of Cl^- -base transport rates.

Effect of H_2DIDS on Cl^- -base exchange in CCD intercalated cells with bilateral Cl^- -base exchange. To further characterize the CCD intercalated cells with bilateral Cl^- -base exchange, the effect of the stilbene inhibitor H_2DIDS on these transporters was studied in separate experiment. In this protocol, a given intercalated cell was first subtyped functionally by

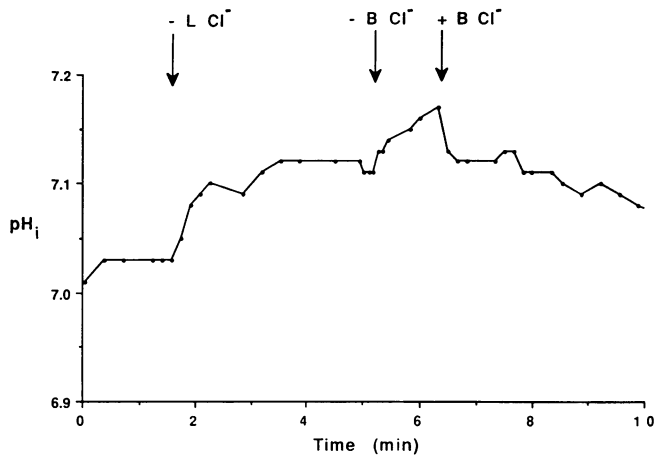


Figure 5. pH_i response to sequential lumen and basolateral Cl^- removal in the presence of $5 \mu M$ valinomycin (lumen and bath). The pH_i response to luminal and basolateral Cl^- removal did not differ from control cells, suggesting that apical and basolateral Cl^- -base exchangers, rather than parallel Cl^- and H^+ -base conductive pathways, account for the results.

Cl^- removal on both sides of the tubule. Then, 0.5 mM H_2DIDS was added to either the lumen or bath for 20 min and the Cl^- removal studies were repeated in the presence of the stilbene inhibitor. Fig. 7 shows the lack of effect of luminal 0.5 mM H_2DIDS on the apical anion exchanger in a representative intercalated cell with bilateral Cl^- -base exchange. Baseline pH_i was 6.79 . Removal of lumen Cl^- caused alkalization to pH_i 6.95 . Cl^- was returned to the lumen and 0.5 mM H_2DIDS was added for 20 min. Then, luminal Cl^- was again removed, with a similar degree of alkalization resulting. The additional alkalization in response to removal of bath Cl^- indicates that this intercalated cell was one with bilateral Cl^- -base exchange. Simi-

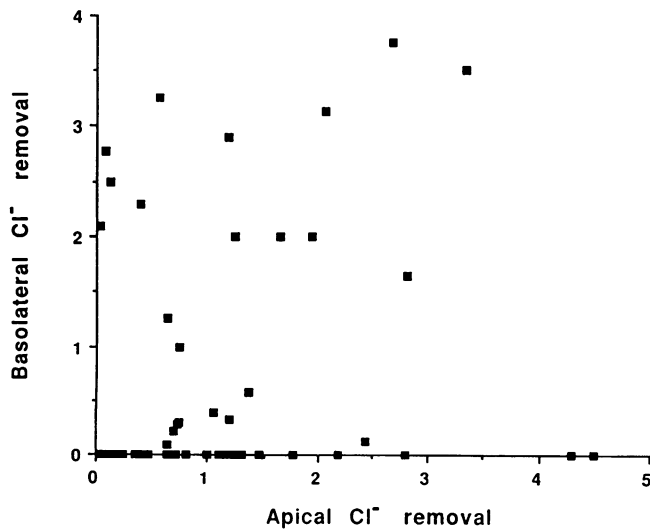


Figure 6. dpH_i/dt in response to luminal Cl^- removal (x axis) vs. that observed with subsequent basolateral Cl^- removal (y axis) in individual intercalated cells. Rather than a clustering of values into two clearly separated groups, a wide range of results is evident. Note the paucity of α cells with only basolateral Cl^- -base exchange.

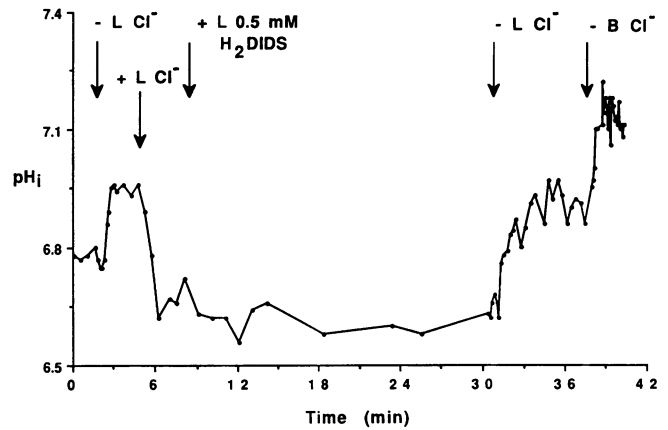


Figure 7. pH_i response of a γ intercalated cell in response to luminal Cl^- removal before and after the addition of 0.5 mM luminal H_2DIDS . There was no effect on the intracellular alkalization resulting from removal of lumen Cl^- after 20-min exposure to 0.5 mM luminal H_2DIDS .

lar studies in 40 intercalated cells (11 tubules) with bilateral Cl^- -base exchange revealed no difference in either the rates of alkalization in response to removal of lumen Cl^- after stilbene exposure or the resultant ΔpH_i values (dpH_i/dt 1.11 ± 0.08 vs. 0.96 ± 0.10 , ΔpH_i 0.35 ± 0.02 vs. 0.31 ± 0.04 , paired, NS). These results demonstrate that the apical anion exchanger in CCD intercalated cells with bilateral anion exchange is not H_2DIDS -sensitive.

Fig. 8 shows the lack of effect of basolateral H_2DIDS on the basolateral Cl^- -base exchanger in an intercalated cell with bilateral Cl^- -base exchange. Removal of lumen Cl^- caused pH_i to increase, followed by a further cell alkalization after removal of basolateral Cl^- . After 20 min of H_2DIDS exposure on the basolateral side, sequential Cl^- removal was repeated, with no effect on the resulting degree of alkalization. Similar studies in nine intercalated cells with bilateral Cl^- -base exchange from seven tubules revealed no difference in either the rates of alkalization in response to removal of basolateral Cl^- after stil-

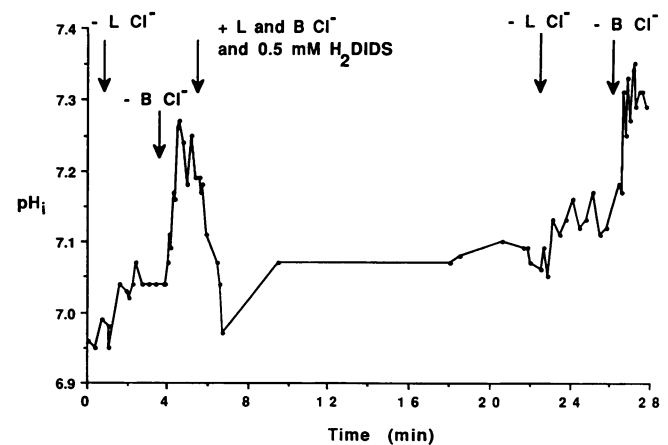


Figure 8. pH_i response of a γ intercalated cell in response to basolateral Cl^- removal before and after 0.5 mM basolateral H_2DIDS . The intracellular alkalization due to removal of bath Cl^- was unchanged after 20-min exposure to 0.5 mM basolateral H_2DIDS .

bene exposure or the resultant $\Delta p\text{H}_i$ values ($dp\text{H}_i/dt$ 0.75 ± 0.19 vs. 0.95 ± 0.30 , $\Delta p\text{H}_i$ 0.12 ± 0.02 vs. 0.15 ± 0.03 , paired, NS). These results demonstrate that the basolateral anion exchanger in CCD intercalated cells with bilateral anion exchange is not H_2DIDS -sensitive.

Lectin binding in CCD intercalated cells. Binding of peanut lectin to the apical membrane has been used as a marker for the classic β intercalated cell model (3, 9, 13). In eleven separate tubules, experiments were done to determine whether intercalated cells with bilateral Cl^- -base exchange bind peanut lectin. The tubules were initially perfused with $50 \mu\text{g/ml}$ FITC-peanut lectin and cells exhibiting apical peanut lectin binding were identified as seen in Fig. 9. Then, the perfusate was changed to one containing BCECF-AM. After dye loading, Cl^- was removed sequentially from the apical and basolateral sides of the tubule, as described previously. Of 44 CCD intercalated cells that bound apical peanut lectin, 48% had only apical anion exchange and 52% had both apical and basolateral anion exchange. Thus, CCD intercalated cells with bilateral Cl^- -base exchange do bind lectin. Therefore, apical peanut lectin binding is not a specific marker for intercalated cells with exclusively apical Cl^- -base exchange (β cells).

Pattern of Cl^- -base exchange among CCDs. The ability to study several intercalated cells simultaneously in the same tubule permitted comparison of intercalated cell Cl^- -base exchange patterns within a given tubule along a $250\text{-}\mu\text{m}$ length. Of 49 tubules in which 4 to 7 intercalated cells were studied, 41% of these tubules had intercalated cells with only one pattern of anion exchange. Fig. 10 illustrates the distribution of anion exchange in intercalated cells of individual tubules with either four, five, six, or seven intercalated cells studied in each tubule. Of those tubules with only one pattern of intercalated cell anion exchange, 35% of the tubules had exclusively intercalated cells with apical anion exchange (β cells) and 65% of the tubules had exclusively intercalated cells with both apical and

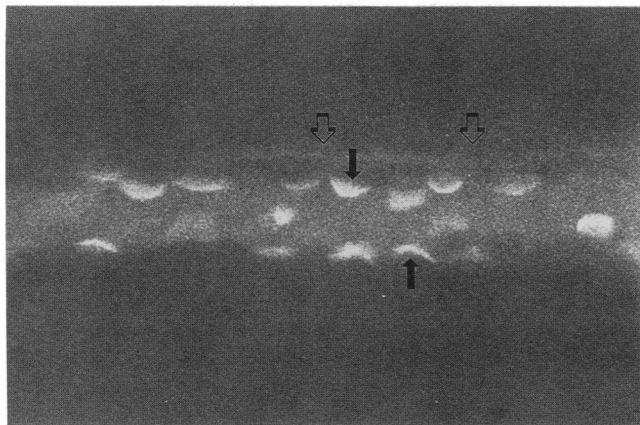


Figure 9. Fluorescent image of a cortical collecting duct after luminal perfusion with $50 \mu\text{g/ml}$ FITC-peanut lectin. After identification of intercalated cells that bound lectin to their apical membrane, the tubule was luminally loaded with BCECF-AM, and Cl^- -base exchange was assessed on both sides of the tubule. In this tubule, cells between the open arrows were studied. Cells designated by a dark arrow exhibited both apical and basolateral $\text{Cl}^-/\text{HCO}_3^-$ exchange (γ cells), while the remaining cells had only apical $\text{Cl}^-/\text{HCO}_3^-$ exchange (β cells).

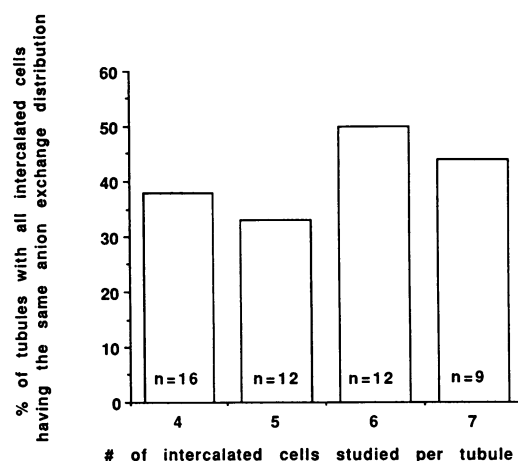


Figure 10. Percentage of tubules with four to seven intercalated cells demonstrating the same anion exchange distribution. The x axis indicates the number of cells studied in a $250\text{-}\mu\text{m}$ length of an individual tubule. The number within the bars indicates the number of tubules studied. The same distribution of intercalated cell anion exchange was seen in 38% of the 16 CCDs with 4 intercalated cells studied per tubule, 33% of the 12 CCDs with 5 intercalated cells studied per tubule, 50% of the 12 CCDs with 6 intercalated cells studied per tubule, and 44% of the 9 CCDs with 7 intercalated cells studied per tubule. Taken together, an average of 41% of all these CCDs (49 tubules) had the same distribution of intercalated cell anion exchange.

basolateral anion exchange (γ cells). The finding that there are CCDs with one intercalated cell type may account for transepithelial H^+ -base and Cl^- transport differences that exist among CCDs dissected from the same level in the outer cortex.

Discussion

Intercalated cells in the CCD are presently divided into two subtypes: α and β cells. The purpose of the present study was to functionally characterize the distribution of Cl^- -base exchange activity in single rabbit intercalated cells in the outer CCD. Cl^- -base exchange activity was documented by the $p\text{H}_i$ responses to sequential removal of apical and basolateral Cl^- in the same cell. The approach allowed a functional determination of whether the traditional subdivision of intercalated cell subtypes into two categories has been overly simplistic. The results demonstrate that the majority of intercalated cells from the rabbit outer CCD have both apical and basolateral Na^+ -independent Cl^- -base exchangers that are stilbene-insensitive. In keeping with the nomenclature given initially to the carbonic anhydrase-rich cells of the turtle bladder, and then extended to CCD intercalated cells on the basis of morphologic similarities, (3, 24, 27) we propose that the newly identified CCD intercalated cells with bilateral Na^+ -independent $\text{Cl}^-/\text{HCO}_3^-$ exchangers be called γ cells. Whether these cells also exist in the turtle bladder is unknown. In addition, intercalated cells with only basolateral Cl^- -base exchange (α cells) are very uncommon in the rabbit outer CCD. Intercalated cells with exclusively apical Cl^- -base exchange (β cells) and cells with bilateral Cl^- -base exchange (γ cells) were both found to bind peanut lectin on the apical membrane. Surprisingly, a large percentage of CCDs had intercalated cells of only one subtype.

One scientific concern must be addressed regarding the use of Na^+ -free solutions in this study. It is possible that the magnitude of anion exchange could be decreased due to the lower pH_i in the presence of zero Na^+ solutions. A Na^+ -free protocol was chosen because the purpose of this study was to examine Na^+ -independent Cl^- -base exchange. In the presence of Na^+ , other Na^+ -dependent transport processes could minimize pH_i changes. It is unlikely that either apical or basolateral Cl^- -base exchange was significantly underestimated in this study for the following reasons. 96% of the 309 intercalated cells studied demonstrated apical anion exchange. Therefore, in only 4% of the 309 intercalated cells would apical anion exchange have been missed. If basolateral anion exchange was missed, the percentage of γ cells would be even greater than 57%. However, it is unlikely that basolateral anion exchange was underestimated due to a low pH_i effect since, after luminal Cl^- removal, the starting pH_i increased to ~ 7.20 before basolateral Cl^- removal. Taken together, it is unlikely that in Na^+ -containing solutions, the percentages of intercalated cell subtypes would have varied significantly from the results reported in this study.

Although, intercalated cells have been traditionally divided into two distinct subgroups, several recent studies have identified intercalated cells that do not fit into the conventional categories of α and β . Based on cellular morphology from transmission electron microscopy, Ridderstrale and colleagues were unable to divide rabbit CCD intercalated cells into two distinct groups, but noted several ultrastructural manifestations that had "subtle and gradual differences, with many intermediate variations" (14). Using antibodies against band 3 and H^+ ATPase, Alper et al. found that 1% of rat intercalated cells had apical H^+ ATPase staining with no band 3 labeling (15). Schwartz et al. characterized intercalated cells in perfused rabbit CCDs with 6-carboxyfluorescein (6-CF) uptake, peanut lectin binding, and luminal endocytosis, and found 5 categories of cells: 6-CF positive only, 6-CF and lectin positive (consistent with the β cell model), 6-CF and endocytosis positive (consistent with the α cell model), lectin positive only, and endocytosis positive only (29). A similar study by Schuster and co-workers combined lectin binding and antibodies against H^+ ATPase and band 3 to identify subtypes of rabbit intercalated cells and found that 75% of intercalated cells had diffuse H^+ ATPase staining with either weak or bright apical lectin caps, consistent with the classical β cell model. However, 13% had apical H^+ ATPase with bright apical lectin caps, 5% had diffuse H^+ ATPase with no lectin binding, and 4% had bright lectin staining with no H^+ ATPase. Only 2% of cells had staining characteristics compatible with the current α cell model, apical H^+ ATPase staining with no lectin binding (16). More recently, Bastani et al. identified six patterns of H^+ ATPase immunocytochemistry in rat CCD intercalated cells: well-polarized apical staining, poorly polarized apical staining, diffuse, apical and basolateral, poorly polarized basolateral staining, and well polarized basolateral staining (17). The present results provide the first functional evidence for an intercalated cell that does not fit the classic α or β cell models. That the number of CCD intercalated cells with bilateral Cl^- -base exchange (γ cells) identified by pH_i measurements is greater than the number of "hybrid" cells found in the immunocytochemical studies may result from the lack of a suitable immunocytochemical marker for the apical Cl^- -base exchanger.

The direction in which HCO_3^- is transported by the CCD is

known to be a function of the in vivo acid-base status of the animal (18). Based on the traditional intercalated cell models, the Cl^- -base exchanger and H^+ ATPase in α and β intercalated cells are present on opposite cell membranes. Some authors have proposed that α and β cells can reverse their polarity and interconvert, causing a change in the direction of HCO_3^- transport (3). Remodeling of the apical membrane with endocytotic removal of the apical Cl^- - HCO_3^- exchanger of β cells has been demonstrated in response to an in vitro acid incubation, although development of new basolateral transport systems was not investigated in this study (19). Thus, reversal of functional polarity of intercalated cells was not demonstrated.

There is evidence that suggests that α and β intercalated cells are distinct cell types which do not interconvert. The apical membrane of either rabbit or rat intercalated cells is not labeled with band 3 antibodies, while the basolateral membrane of some intercalated cells does label with antibodies to band 3 (9). HCO_3^- reabsorption in rabbit CCDs (presumably an α cell function) is blocked by basolateral stilbene inhibitors, but apical stilbenes do not inhibit HCO_3^- secretion (attributed to β cells) as reported by Schuster (20). Differences have also been noted in carbonic anhydrase II staining between type A and type B rat CCD intercalated cells (22). Recently, Satlin and Schwartz found a decrease in net CCD HCO_3^- secretion in response to an in vitro acid incubation, but no change in HCO_3^- absorption, suggesting that reversal of functional polarity did not occur between α and β cells (23). The identification of γ intercalated cells in the present study makes the issue of reversal of polarity and/or remodeling of α and β intercalated cells even more complex.

That the rate of apical vs. basolateral Cl^- -base exchange varies widely among γ cells under control conditions (see Fig. 6) suggests the possibility that these cells, as a population, may not have a uniform contribution to transepithelial H^+ -base transport. The cell currently felt to be responsible for CCD HCO_3^- secretion, the β cell, shares several characteristics with the γ cell. CCD HCO_3^- secretion is unaffected by luminal stilbenes (20). The apical Cl^- - HCO_3^- exchanger of β and γ intercalated cells is not inhibited by stilbenes. In addition, the apical membrane of both cell types binds peanut lectin. These similarities suggest the possibility that both cells may contribute to CCD HCO_3^- secretion. A γ cell could mediate HCO_3^- secretion if its apical Cl^- - HCO_3^- exchanger functioned at a greater rate than its basolateral Cl^- - HCO_3^- exchanger and if other transport processes (i.e., H^+ ATPase) mediated efflux of acid-equivalents across the basolateral membrane.

Immunocytochemical studies suggest that $\sim 30\%$ of rabbit CCD intercalated cells are of the α subtype (9). Using luminal endocytosis as an α cell probe, Schwartz et al. found that 21% of intercalated cells in the rabbit mid CCD were α cells (20). However, the present studies suggest that cells with only basolateral Cl^- -base exchange, consistent with the traditional α cell model, are much less common in the rabbit outer CCD. This is in keeping with the findings of Weiner and Hamm, although the anatomical location of the CCDs examined was not specified (21). As such, the cell responsible for HCO_3^- absorption in the rabbit CCD is not known at present. A γ cell could mediate HCO_3^- absorption if the basolateral Cl^- -base rate exceeded the apical rate, and if an apical transport pathway for efflux of acid-equivalents is also present. In the proximal tubule, both the apical and basolateral membranes have Na^+ -independent

Cl⁻-base exchangers. Net HCO₃⁻ absorption is mediated by other apical H⁺ efflux and basolateral base efflux pathways (28). Whether similar transport processes are present on the γ cell is yet to be determined. Against the notion that γ cells mediate HCO₃⁻ absorption is the finding that the basolateral exchanger of these cells is unaffected by stilbenes. CCD HCO₃⁻ absorption, however, is stilbene sensitive. Further studies are needed to distinguish the pH_i regulatory role, the volume regulatory role, and the transepithelial H⁺-base transport function of the apical and basolateral anion exchangers in γ cells.

Previous reports of variability in CCD Cl⁻ tracer flux have been attributed to axial heterogeneity of intercalated cell subtypes along the rabbit CCD. β intercalated cells are thought to provide the major pathway for CCD transepithelial Cl⁻ transport and are more common in the outer cortex, the region where Cl⁻ tracer flux is greater (11, 24). However, another explanation is provided by the finding in the present study that, in many CCDs, the intercalated cells are all of the same subtype. It is feasible that similar H⁺-base transport properties among intercalated cells in the same tubule account for whole tubule H⁺-base transport differences. The mechanism(s) of intertubule heterogeneity is not clear. Differences in CO₂ tension are not a likely explanation, given the known axial gradient of CO₂ in the cortex (25, 26). In addition, it is unlikely that local hormonal differences could exist between individual tubules within the cortex. Further studies are required to better understand this phenomenon of interCCD heterogeneity.

In summary, the majority of rabbit outer CCD intercalated cells (γ cells) have both apical and basolateral Cl⁻-HCO₃⁻ exchangers which are stilbene insensitive. Apical peanut lectin binds to both β cells and γ cells. In addition, in many rabbit outer CCDs, intercalated cells in a given tubule are of the same subtype, suggesting the presence of intertubule heterogeneity.

Acknowledgments

This work was supported by a Veterans Affairs Career Development Research Associate Award (to C. Emmons) and by a National Institutes of Health grant (851-IG-4 to I. Kurtz). Dr. Kurtz is an Established Investigator of the American Heart Association.

References

- Madsen, K. M., and C. C. Tisher. 1986. Structural-functional relationships along the distal nephron. *Am. J. Physiol.* 250:F1-F15.
- Star, R. A., M. B. Burg, and M. A. Knepper. 1985. Bicarbonate secretion and chloride absorption by rabbit cortical collecting duct. Role of chloride/bicarbonate exchange. *J. Clin. Invest.* 76:1123-1130.
- Schwartz, G. J., J. Barasch, and Q. Al-awqati. 1985. Plasticity of functional polarity. *Nature (Lond.)*. 318:368-371.
- Sansom, S. C., E. J. Weinman, and R. G. O'Neil. 1984. Microelectrode assessment of chloride-conductive properties of cortical collecting duct. *Am. J. Physiol.* 247:F291-F293.
- Koeppen, B. M., B. A. Biagi, and G. H. Giebisch. 1983. Intracellular microelectrode characterization of the rabbit cortical collecting duct. *Am. J. Physiol.* 244:F35-F47.
- Brown, D., S. Hirsh, and S. Gluck. 1988. An H⁺-ATPase in opposite plasma domains in kidney epithelial cell subpopulations. *Nature (Lond.)*. 331:622-624.
- Muto, S., K. Yasoshima, K. Yoshitomi, M. Imai, and Y. Asano. 1990. Electrophysiological identification of α and β intercalated cells and their distribution along the rabbit distal nephron segments. *J. Clin. Invest.* 86:1829-1839.
- Furuya, H., M. D. Breyer, and H. R. Jacobson. 1991. Functional characterization of α and β intercalated cell types in rabbit cortical collecting duct. *Am. J. Physiol.* 261:F377-F385.
- Schuster, V. L., S. M. Bonsib, and M. L. Jennings. 1986. Two types of collecting duct mitochondria-rich (intercalated cells):lectin and band 3 cytochemistry. *Am. J. Physiol.* 251:C347-C355.
- Wang, X., and I. Kurtz. 1990. H⁺/base transport in principal cells characterized by confocal fluorescence imaging. *Am. J. Physiol.* 259:C365-C373.
- Emmons, C., K. Matsuzaki, J. B. Stokes, and V. L. Schuster. 1991. Axial heterogeneity of rabbit cortical collecting duct. *Am. J. Physiol.* 260:F498-F505.
- Weiner, I. D., and L. L. Hamm. 1989. Use of fluorescent dye BCECF to measure intracellular pH in cortical collecting tubule. *Am. J. Physiol.* 256:F957-F964.
- LeHir, M., B. Kaissling, B. M. Koeppen, and J. B. Wade. 1982. Binding of peanut lectin to specific epithelial cell types in kidney. *Am. J. Physiol.* 244:F289-F296.
- Ridderstrale, Y., M. Kashgarian, B. Koeppen, G. Giebisch, D. Stetson, T. Ardito, and B. Stanton. 1988. Morphological heterogeneity of the rabbit collecting duct. *Kidney Int.* 34:655-670.
- Alper, S. L., J. Natale, S. Gluck, H. F. Lodish, and D. Brown. 1989. Subtypes of intercalated cells in rat kidney collecting duct defined by antibodies against erythroid band 3 and renal vacuolar H⁺-ATPase. *Proc. Natl. Acad. Sci. USA.* 86:5229-5433.
- Schuster, V. L., G. Fejes-Toth, A. Naray-Fejes-Toth, and S. Gluck. 1991. Colocalization of H⁺-ATPase and band 3 exchanger in rabbit collecting duct intercalated cells. *Am. J. Physiol.* 260:F506-517.
- Bastani, B., H. Purcell, P. Hemken, D. Trigg, and S. Gluck. 1991. Expression and distribution of renal vacuolar proton-translocating adenosine triphosphatase in response to chronic acid and alkali loads in the rat. *J. Clin. Invest.* 88:126-136.
- McKinney, T. D., and M. B. Burg. 1977. Bicarbonate transport by rabbit cortical collecting tubules. Effect of acid and alkali loads in vivo on transport in vitro. *J. Clin. Invest.* 60:766-768.
- Satlin, L. M., and G. J. Schwartz. 1989. Cellular remodeling of HCO₃⁻ secreting cells in rabbit renal collecting duct in response to an acidic environment. *J. Cell Biol.* 109:1279-1288.
- Schuster, V. L. 1985. Cyclic adenosine monophosphate-stimulated bicarbonate secretion in rabbit cortical collecting tubules. *J. Clin. Invest.* 75:2956-2964.
- Weiner, I. D., and L. L. Hamm. 1990. Regulation of intracellular pH in the rabbit cortical collecting tubule. *J. Clin. Invest.* 85:274-281.
- Kim, J., C. C. Tisher, P. J. Linser, and K. M. Madsen. 1990. Ultrastructural localization of carbonic anhydrase II in subpopulations of intercalated cells of the rat kidney. *J. Am. Soc. Nephrol.* 1:245-256.
- Satlin, L. M., and G. J. Schwartz. 1992. Adaptation of rabbit cortical collecting duct to in vitro acid incubation. *Am. J. Physiol.* 263:F749-F756.
- Schuster, V. L., and J. B. Stokes. 1987. Chloride transport by the cortical and outer medullary collecting duct. *Am. J. Physiol.* 253:F203-F212.
- Atherton, L. J., D. A. Maddox, F. J. Gennari, and W. M. Deen. 1988. Analysis of pCO₂ variations in the renal cortex. I. Single nephron. *Am. J. Physiol.* 255:F349-F360.
- Atherton, L. J., D. A. Maddox, F. J. Gennari, and W. M. Deen. 1988. Analysis of pCO₂ variations in the renal cortex. II. Countercurrent exchange. *Am. J. Physiol.* 255:F361-F371.
- Stetson, D. L., and P. R. Steinmetz. 1985. α and β types of carbonic anhydrase-rich cells in turtle bladder. *Am. J. Physiol.* 249:F553-F565.
- Berry, C. A., and F. C. Rector, Jr. 1991. Mechanism of proximal NaCl reabsorption in the proximal tubule of the mammalian kidney. *Semin. Nephrol.* 11:86-97.
- Schwartz, G. J., L. M. Satlin, and J. E. Bergmann. 1988. Fluorescent characterization of collecting duct cells: a second H⁺-secreting type. *Am. J. Physiol.* 255:F1003-1014.